Aerosol and Air Quality Research, 18: 1366–1374, 2018

ISSN: 1680-8584 print / 2071-1409 online
doi: 10.4209/aaqr.2017.11.0458

Effect of Aerosol Loading on Separation Performance of $PM_{2.5}$ Cyclone Separators

Chih-Wei Lin[1], Ting-Ju Chen[1], Sheng-Hsiu Huang[1], Yu-Mei Kuo[2*], Hua-Qiao Gui[3], Chih-Chieh Chen[1]

[1] *Institute of Occupational Medicine and Industrial Hygiene, College of Public Health, National Taiwan University, Taipei 10055, Taiwan*
[2] *Department of Occupational Safety and Health, Chung Hwa University of Medical Technology, Tainan 71703, Taiwan*
[3] *Anhui Institute of Optics and Fine Mechanics, Chinese Academy of Sciences, Hefei 230031, China*

ABSTRACT

The adverse health effects of particulate matter less than 2.5 μm in diameter ($PM_{2.5}$) have drawn increasing attention over the past several decades. To obtain reliable measurements, it is critical to efficiently separate $PM_{2.5}$ in the airstream from the beginning till the end of sampling. However, commonly used separators for $PM_{2.5}$ monitoring, such as the BGI Very Sharp Cut Cyclone (VSCC), are usually subject to aerosol-loading effects. This study investigates the loading effect on cyclone separation performance as a function of particle size, cyclone size, particle material, and air humidity. Based on the ratios of dimensions to the body diameter of the BGI VSCC, four cyclones with different body diameters (13–35.6 mm) were fabricated. An ultrasonic atomizer was employed to generate micrometer-sized potassium sodium tartrate (PST) particles and sodium chloride (NaCl) particles as solid challenge particles and di-ethyl-hexyl-sebacate (DEHS) particles as liquid ones. Aerosol particles were neutralized to the Boltzmann charge equilibrium. An aerodynamic particle sizer measured the aerosol distributions and number concentrations upstream and downstream of the cyclones. The experimental results show that solid particles such as PST with sizes close to the cyclone cut-point exhibit a significant loading effect. However, no significant difference is found due to the aerosol loading effect on four different-sized cyclones. The cyclone separation curve appears to shift toward smaller sizes due to aerosol loading. During the loading test, the aerosol penetration of 2.5-μm particles abruptly decreased during the first 20 minutes from 50% to a relatively stable level at 30%—an average decrease of 20%. Thus, the performance of cyclone $PM_{2.5}$ samplers with progressive aerosol loading might result in an underestimation of $PM_{2.5}$, particularly for continuous monitoring.

Keywords: Aerosol loading; Size-selective separator; Cyclone; Continuous aerosol monitoring.

INTRODUCTION

Particulate matter has been considered a critical health issue for several decades (Dockery *et al*., 1993; Kim, 2015). Recently, more attention has been drawn to related adverse health effects as a function of particle size, particularly with particulate matter less than or equal to 2.5 μm, i.e., $PM_{2.5}$, or fine particulate matter (Dominici *et al*., 2006; Ostro *et al*., 2006; Zanobetti *et al*., 2009; Xing *et al*., 2016). To regulate $PM_{2.5}$, it is crucial to accurately and constantly separate $PM_{2.5}$ from the sampled air stream to gain reliable $PM_{2.5}$ measurements. Two types of particle separators are commonly used for size-selective aerosol sampling, the impactor and the cyclone (Okuda *et al*., 2015). It is generally known that the performance of impactors is affected by particle bounce and overloading, especially over a long sampling time period. For the two major types of $PM_{2.5}$ separators approved by USEPA, the well-type impactor ninety-six (WINS) Impactor and the Very Sharp Cut Cyclone (VSCC), the VSCC surpasses the WINS Impactor in continuous particulate monitoring (CPM) for superior performance over long sampling periods under heavy loading (Kenny *et al*., 2004).

However, similar to the WINS impactor, VSCC separator also displays reduced particle penetration as a function of aerosol loading (Kenny *et al*., 2004). It is speculated that the performance of cyclone separators is less sensitive to loading levels than that of impactors due to the larger deposition area of the cyclones (Vanderpool *et al*., 2001). Some studies have confirmed the loading effect on the performance of the commonly used 10-mm nylon cyclone for workplace respirable sampling (Blachman and Lippmann, 1974; Tsai *et al*., 1999). Blachman and Lippmann (1974) found the accumulated dust on the cyclone wall opposite

*Corresponding author.
Tel.: 886-912017249; Fax: 886-2-23938631
E-mail address: ymkuo@mail.hwai.edu.tw

the inlet gradually reduced the effective diameter of the cyclone when sampling highly concentrated dust and that the cyclone efficiency accordingly increased with increasing velocity at the point of particle deposit. Tsai *et al*. (1999) conjectured that the presence of previously deposited particles was responsible for absorbing a portion of the incident particle's kinetic energy, thus reducing particle penetration versus loading. Previous study demonstrated the separation performance of a respirable 10-mm nylon cyclone can deteriorate with progressive particle loading and the loading effect can be strongly dependent on both particle type and size (Chen and Huang, 1999).

Cyclone separation performance is also significantly affected by cyclone geometry (Hsu *et al*., 2014; Kenny *et al*., 2017). The work of Kenny and Gussman demonstrated that cyclones can be dimensionally scaled and the cyclone cut point can be estimated by the cyclone body diameter and flow rate. In addition, certain geometrical parameters, such as the cone shape, grit pot diameter, inlet and vortex outlet dimensions were also found to influence the cyclone cut-point, but not the slope of the penetration curves (Kenny and Gussman, 1997). Because of the complexity of gas flow pattern in a cyclone, many experimental and theoretical studies sought to develop models to describe its performance (Moore and McFarland, 1993; Lidén and Gudmundsson, 1997; Hsiao *et al*., 2015; Kenny *et al*., 2017). However, all of these models can only predict the performance of cyclones without particle loading on the inner wall. Since the VSCC™ is claimed to require cleaning at infrequent intervals (Kenny *et al*., 2004), we fabricated a family of VSCCs with different cyclone sizes to accommodate different flow rate requirements for $PM_{2.5}$ separation in order to thoroughly study the characteristics of aerosol loading effect on the cyclone separation performance.

METHODS

Fig. 1 shows a schematic diagram of the experimental system set-up. An ultrasonic atomizer (Model 8700-120MS, Sono-Tek Corporation, Poughkeepsie, NY, USA) was used to generate micrometer-sized DEHS (di-ethyl-hexyl-sebacate, density 0.916 g cm^{-3}, technical grade 90%, Sigma-Aldrich, St. Louis, MI, USA, product number 290831) particles as liquid challenge aerosols, NaCl (sodium chloride, density 2.17 g cm^{-3}, purity ≥ 99.5%, Wako Pure Chemical Industries, Ltd., Osaka, Japan) and PST (potassium sodium tartrate tetrahydrate, density 1.79 g cm^{-3}, $KOCO(CHOH)_2COONa{\cdot}4H_2O$, A.C.S. grade, J.T.Baker®, Center Valley, PA, USA) particles as solid challenge aerosols. A syringe pump (KDS 200/200P, KD Scientific Inc., Holliston, MA, USA) delivered the solution to the ultrasonic atomizer to generate challenge particles with the desired number concentrations and aerosol size distributions by adjusting the liquid delivery rate and the solution concentration.

Particles with count median diameters (CMDs) of 3, 7 and 10 μm were generated to evaluate the loading characteristics of the cyclones as a function of particle size. An aerosol neutralizer (25-mCi Po-210 radioactive source) was used to neutralize the particles to the Boltzmann charge equilibrium. The aerosol output was diluted with filtered air and then introduced into the test chamber. The test chamber was 20 cm in diameter and 150 cm in height. The relative humidity (RH) of the incoming compressed air was around 10%. The total dilution flow rate was 80 L min^{-1} and the corresponding average air velocity in the test

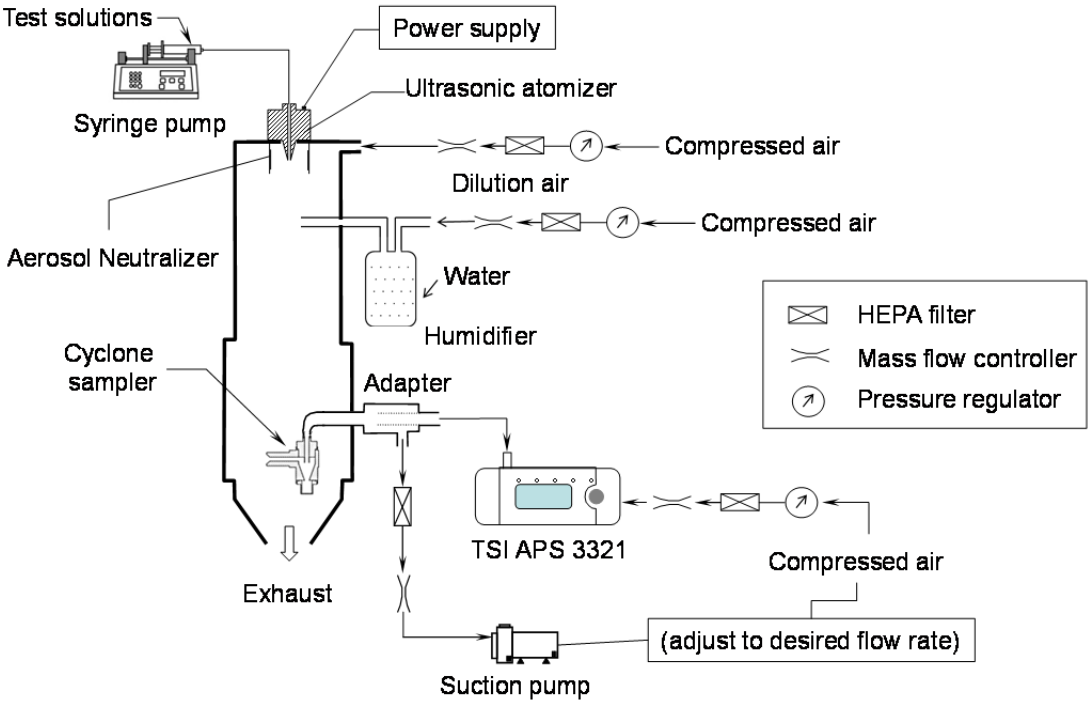

Fig. 1. Schematic diagram of the experimental system.

chamber was about 4.3 cm s^{-1}. The RH inside the test chamber was about 20% unless otherwise specified. For the humidity experiments, a humidifier was used to adjust the air humidity inside the test chamber from 20% to 90% to evaluate the humidity effect on the aerosol loading characteristics. All the air flow rates were controlled by mass flow controllers (Model HFM 201 & HFC 202, Teledyne Hastings Instruments, Hampton, VA, USA).

In this study, different sizes of cyclones were used to evaluate the effect of the cyclone size on the loading characteristics. Each cyclone operates at a different flow rate but has the same size cutoff size of 2.5 µm. To have a 2.5-µm cut-point, the operating flow rate of the cyclone was estimated using the VSCC family model developed by Kenny *et al*. (2004).

$$\ln(D_{50}) = a + b\ln(D) - (b - 1)\ln(Q) \quad (1)$$

where D_{50} is 2.5 µm, D is the inner diameter of the cyclone body in cm, Q is the flow rate in L min^{-1}, a = 1.415 and b = 1.908. Nevertheless, the actual flow rates for the self-made PM 2.5 cyclone separators were determined by laboratory test.

Based on the dimensionless ratios of a commercially available USEPA VSCC PM 2.5 separator (VSCC™-A $PM_{2.5}$, S/N 200411-69, BGI Inc., Waltham, MA, USA), a family of VSCCs with body diameter varying from 13.0 to 35.6 mm were fabricated with aluminum as shown in Fig. 2. The self-made VSCC $PM_{2.5}$ separators accommodated the operating flow rate from 4 to 26.5 L min^{-1}. The specifications of the four self-made VSCC $PM_{2.5}$ separators is summarized in Table 1. It should be noted that the VSCC III is a replica of BGI VSCC™-A. Unless otherwise specified, all the loading experiments were conducted with a self-made $PM_{2.5}$ separator (VSCC III). The test parameters are listed in Table 2.

An aerodynamic particle sizer (APS, Model 3321, TSI Inc., St. Paul, MN, USA) was used to measure the particle size distributions and number concentrations upstream and downstream of the cyclones in the aerodynamic size ranges of 0.5–20 µm. The aerosol penetration through the tested cyclone was determined by the ratio of downstream to upstream particle number concentrations at a given particle size. For all experiments, each measurement was conducted with 5 replications.

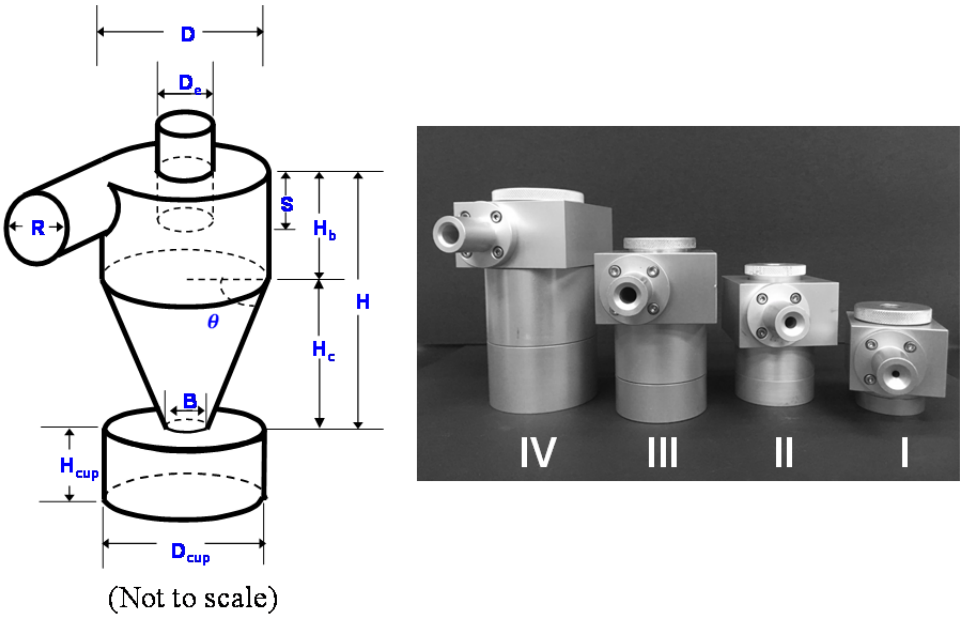

Fig. 2. Schematic diagram and image of the self-made $PM_{2.5}$ separators.

Table 1. Specifications of self-made VSCC $PM_{2.5}$ separators.

		VSCC I	VSCC II	VSCC III	VSCC IV
Sampling flow rate, Q (L min^{-1})		4.0	11.5	16.7	26.5
Body diameter , D (mm)		13.0	23.0	29.5	35.6
Vortex finder diameter, De (mm)	$D_e/D = 0.3$	3.9	6.9	8.9	10.7
Inlet diameter, R (mm)	R/D = 0.28	3.6	6.4	8.2	9.9
Vortex finder length, S (mm)	S/D = 0.69	9.0	15.9	20.4	24.6
Dust outlet, B (mm)	B/D = 0.35	4.5	8.0	10.3	12.4
Body height, H_b (mm)	$H_b/D = 0.65$	8.4	14.9	19.1	23.1
Cone height, H_c (mm)	$H_c/D = 1.29$	16.7	30.0	38.0	45.7
Dust cup hehgit, H_{cup} (mm)	$H_{cup}/D = 0.84$	11.0	19.4	24.9	30.0
Dust cup diameter, D_{cup} (mm)	$D_{cup}/D = 0.61$	7.9	14.0	18.0	21.7

Table 2. List of test parameters.

Parameter	
Particle material	DEHS, NaCl, PST
Count median diameter, CMS (μm)	3, 7, 10
Body diameter, D (mm)	13–35.6
Flow rate, Q (L min^{-1})	4.0–26.5
Relative Humidity, RH (%)	20–90

To evaluate the performance of the aerosol generation system, the filter samples were obtained and the collected particle mass was determined by gravimetric analysis. For KCl particles with CMD of 0.98 μm and GSD of 1.37, the loaded mass concentration (C_{load}, in mg m^{-3}) can be accurately predicted with the feeding rate (Q_{feed}, mL min^{-1}) by the following equation, where the constant 4.757 is the coefficient of the linear regression.

$$C_{load} = 4.757\ Q_{feed} \quad (2)$$

The count data measured by an APS can be transformed into the mass data by assuming the particle density, and the real-time monitoring of the aerosol mass concentration in the test chamber for a prolonged duration of 12 hours demonstrated excellent performance for aerosol production with the coefficient of variance of 7.6%.

RESULTS AND DISCUSSION

Effect of Particle Material on Loading Characteristics

With approximately the same size distribution (CMD of 3 μm and GSD of 1.3), DEHS, NaCl and PST particles were generated to challenge the tested cyclone for one hour. The aerosol penetration curves (initial and after one-hour loading) are plotted in Fig. 3. At the beginning of the loading process, all challenge particles exhibit almost identical aerosol penetration curves. The mass concentrations of DEHS, NaCl and PST particles are 2.7, 3.1 and 3.7 mg m^{-3}, respectively. After one-hour loading under a flow rate of 16.67 L min^{-1}, the corresponding total deposited mass for DEHS, NaCl and PST are 2.8, 3.2 and 3.7 mg, respectively. The reductions of 2.5-μm aerosol penetration for DEHS, NaCl and PST are 1.9 ± 1.2%, 11.2 ± 0.7% and 19.5 ± 1.5%, respectively.

The after-loading 50% cut-points are 2.47, 2.33 and 2.25 μm for DEHS, NaCl and PST, respectively. As expected, the aerosol penetration curves (initial and after one-hour loading) for liquid DEHS particles are almost identical, with no significant change after loading. Particle-surface deformation is the dominating mechanism for absorbing the particle's incoming kinetic energy and this explains why the loading effect of liquid aerosols is negligible. As for the solid particles, the accumulated particle deposits decrease particle penetration efficiency and subsequently shift the separator's cut-point toward the smaller sizes. This is in good agreement with several previous studies on the 10-mm nylon cyclone commonly used for workplace respirable sampling (Blachman and Lippmann, 1974; Chen and Huang, 1999; Tsai *et al*., 1999).

Moreover, the loading effect of the cyclone is more significant for PST particles than for NaCl particles. Particle deposition occurs when the impaction surface is able to completely absorb the kinetic energy of the incident particles. When this happens, the particle is retained by the surface. In contrast to the behavior of liquid particles, the particle-surface interaction of solid particles is more complicated. As the loading proceeds, the layers of previously deposited particles change the nature of the deposition surface and the incident particles impact on previously deposited particles rather than the underlying surface. Eventually, the buildup of deposited particles becomes an obstacle and may perturb the flow pattern. Those particles with lower inertia are accidentally collected on the cyclone wall and bias the separation efficiency of the cyclone toward the smaller aerodynamic sizes. As a result, this may lead to underestimation of $PM_{2.5}$ concentrations, particularly in continuous particulate monitoring. The deposition and re-entrainment of solid particles onto the wall surface of the cyclone is a complex phenomenon. The surface properties of the particles and the roughness of the wall surface can both affect the separation efficiency of a cyclone and play a critical role in the loading characteristics. In addition, the particle shape and size as well as elastic properties, impaction substrate elastic properties, particle incident kinetic energy, amount of surface loading and the relative humidity of the incident airstream are also involved. However, these factors are beyond the scope of this study.

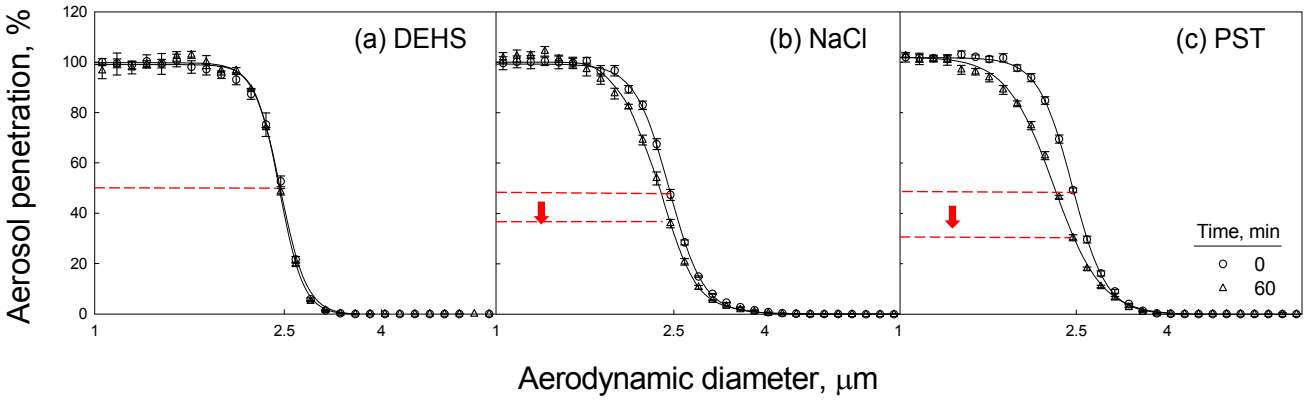

Fig. 3. Separation efficiency curves (initial and after one hour loading) for different kinds of loading particles.

With approximately the same size distribution (CMD of 3 μm and GSD of 1.3), total loaded mass of DEHS, NaCl and PST particles are 2.8, 3.2 and 3.7 mg, respectively. The aerosol penetration of 2.5-μm particles through the cyclone as a function of loading time is shown in Fig. 4. The aerosol penetration of PST particles decreases abruptly as the loading process begins and eventually achieves an equilibrium, in which the aerosol deposition and re-entrainment rates are equal, a phenomenon yet to be investigated further. A similar decreasing trend with less penetration reduction is observed for NaCl particles. No significant change in cyclone cut point is found after one-hour loading of DEHS particles. Since PST particles exhibit a significant loading effect on cyclone separation performance, they are chosen as the challenge aerosols for the following experiments.

Effect of Particle Size on the Loading Characteristics

The initial and after-loading aerosol penetration curves of challenge PST particles with three distinct aerodynamic sizes (CMDs of 3, 7 and 10 μm) are shown in Fig. 5. The concentrations of challenge aerosols are 4.5, 20.0 and 24.5 mg m^{-3} for 3-, 7- and 10-μm PST particles, respectively. Accordingly, the deposited mass yields are 4.4, 19.1 and 22.7 mg for 3-, 7- and 10-μm particles. It is found that the after-loading separation efficiency curves become less sharp and shift to smaller diameters for both 3- and 7-μm particles. Reductions of the 2.5-μm aerosol penetration are 19.5 ± 1.5%, 20.2 ± 1.8% and 8.7 ± 1.7% for 3-, 7- and 10-μm PST particles, respectively. Furthermore, the after-loading cut-points are 2.25, 2.26 and 2.41 μm for 3-, 7- and 10-μm particles, respectively. It is noteworthy that larger particles have less impact on the separation performance of a cyclone, regardless of the higher loaded mass.

To understand why the larger particles with higher loaded mass have less loading effect, the deposition patterns of 3- and 10-μm particles on the inner wall of the cyclone are pictured, as shown in Fig. 6. The upper and lower images show the particle deposition inside the cyclone after being challenged individually with 4.5-mg small particles (CMD of 3 μm and GSD of 1.3) and 24.5-mg large particles

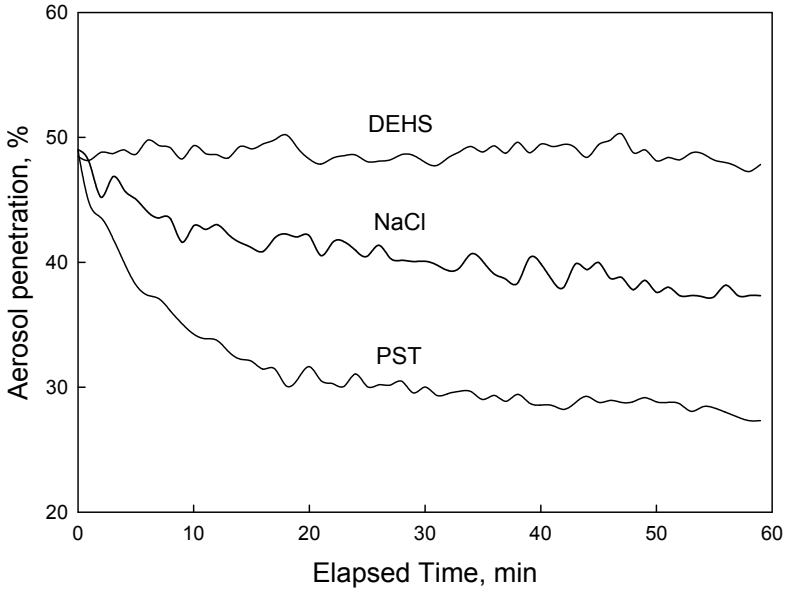

Fig. 4. Penetration of 2.5 μm DEHS, NaCl and PST particles as functions of loading time.

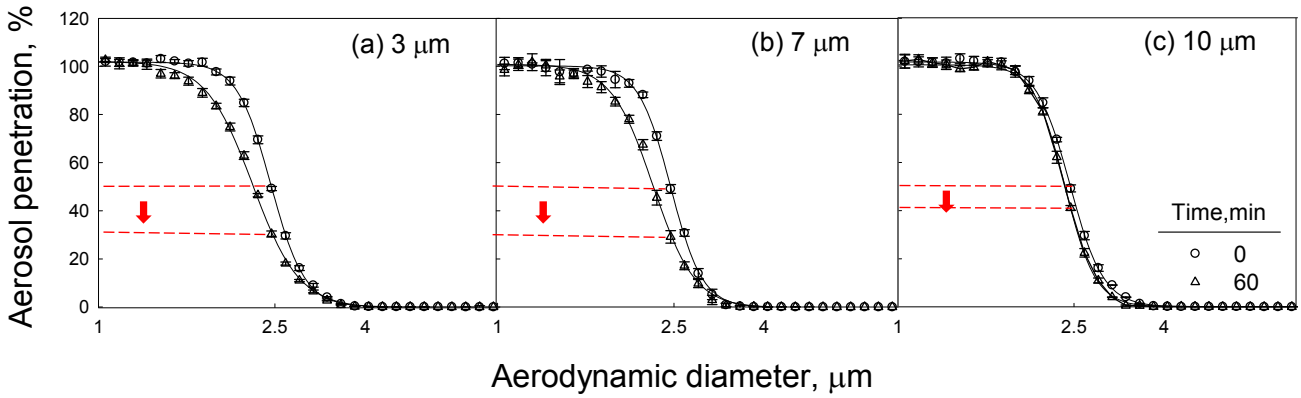

Fig. 5. Separation efficiency curves (initial and after one hour loading) for different sizes of PST particles through a VSCC III sampler.

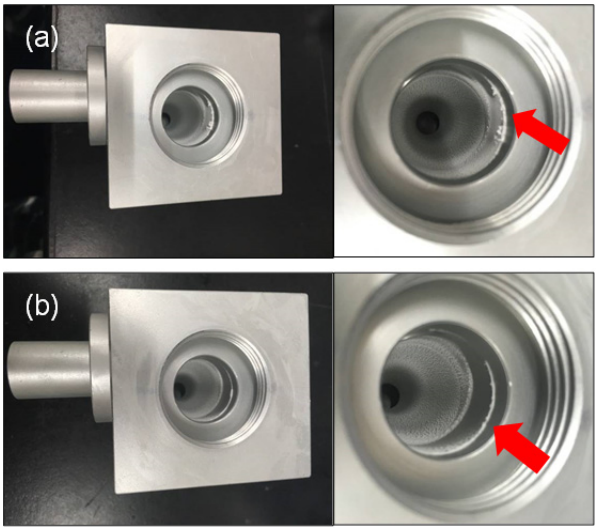

Fig. 6. Deposition patterns of (a) 3 μm and (b) 10 μm PST particles on the inner wall opposite the inlet of the cyclone.

(CMD of 10 μm and GSD of 1.4). When the dust-laden air enters tangentially into the cyclone, the spinning air movement creates centrifugal force and causes particles to move outward onto the side wall of the cyclone. The impact points occur right along the tangential direction of the gas stream. In this instance, the inlet air velocity of the cyclone is fairly high (448 cm s^{-1}). The larger particles with higher momentum hit previously deposited particles and push them further downstream, as indicated in Fig. 6(b) with an arrow mark. As a result of a widening collection area, more particles can be accommodated and their impact on cyclone separation performance is alleviated. On the contrary, the deposition area for smaller particles with lesser momentum is more confined because the incident kinetic energy subsides shortly after the particle-surface collision takes place. This may explain why the loading of small particles has a more drastic impact on the cyclone separation performance.

Effect of Cyclone Size on the Loading Characteristics

To evaluate the effect of cyclone size on the separation performance, four distinct dimensions of self-made cyclones were challenged with 3-μm PST particles at a mass concentration of 4.2 mg m^{-3} for an hour. Fig. 7 shows the initial and after-loading separation efficiency curves for these four cyclones. The aerosol penetration curves become less sharp and a significant deviation from the designated USEPA $PM_{2.5}$ separation curve is found for all tested cyclones. To attain a cut-point of 2.5 μm, the corresponding inlet air velocities are 558, 513, 448 and 491 cm s^{-1} for VSCC I, SVCC II, VSCCIII and VSCC IV, respectively. The total loaded masses are 1.0, 2.7, 4.2 and 6.6 mg and the reductions of the 2.5-μm aerosol penetration are 18.5 ± 1.3%, 19.2 ± 0.7%, 19.5 ± 1.5% and 18.7 ± 1.1% for VSCC I, II, III and IV, respectively. No significant difference on the loading characteristics is found for different-sized cyclones. Moreover, the loading effect on the reduction of aerosol penetration is most profound with particle sizes close to the cut-point of a clean cyclone. The cut-points after one-hour loading shift from 2.5 μm to 2.27, 2.25, 2.25 and 2.20 μm for VSCC I, II, III and IV, respectively.

According to USEPA performance requirements for a FRM $PM_{2.5}$ separator, the D_p50 should be 2.5 ± 0.2 μm (40 CFR part 53). As a worst-case scenario, the cut-point of a clean $PM_{2.5}$ sampler can be as low as 2.3 μm, and furthermore, the separation performance can be soon deteriorated further due to aerosol loading. Therefore, to alleviate the bias due to aerosol loading, the performance requirements might need to be more rigorous, such as 2.5 ± 0.05 μm.

As challenged with 3-μm PST particles at a mass concentration of 4.2 mg m^{-3} for one hour, the aerosol penetration of 2.5-μm particles through the four self-made cyclones as a function of loading time is shown in Fig. 8. Similar decreasing trend is found for the four tested cyclones. The aerosol penetration of 2.5-μm particles decreases abruptly from 50% to approximately 30% and remains relatively constant after loading for 20 minutes. It should be noted that the cyclone separation performance begins to deteriorate as soon as the aerosol loading is initiated. Moreover, a drastic decrease in the aerosol penetration is found even when the loaded mass is low. This implies that the constant operation of size-selective sampling is nearly impossible, because the aerosol penetration curves deviate from the targeted sampling convention immediately after the sampling is activated.

After being loaded for 20 minutes, the cut-points of the cyclones shift from 2.5 μm to 2.33, 2.30, 2.30 and 2.26 μm for VSCC I, II, III and IV, respectively. As a rough estimation, particle loading at a mass concentration of 4.2 mg m^{-3} under a flow rate of 16.67 L min^{-1} for 20 minutes yields a total loaded mass of 1.4 mg which simulates a monitoring time period of 5600 minutes (equivalent to 3 days, 21 hours and 20 minutes) at the annual $PM_{2.5}$ limit value of 15 μg m^{-3} and that of 2400 minutes (equivalent to 1 day and 16 hours) at the 24-hour $PM_{2.5}$ limit value of 35 μg m^{-3}, respectively. Notice that the aerosol mass concentration of 4.2 μg m^{-3} employed in the present study

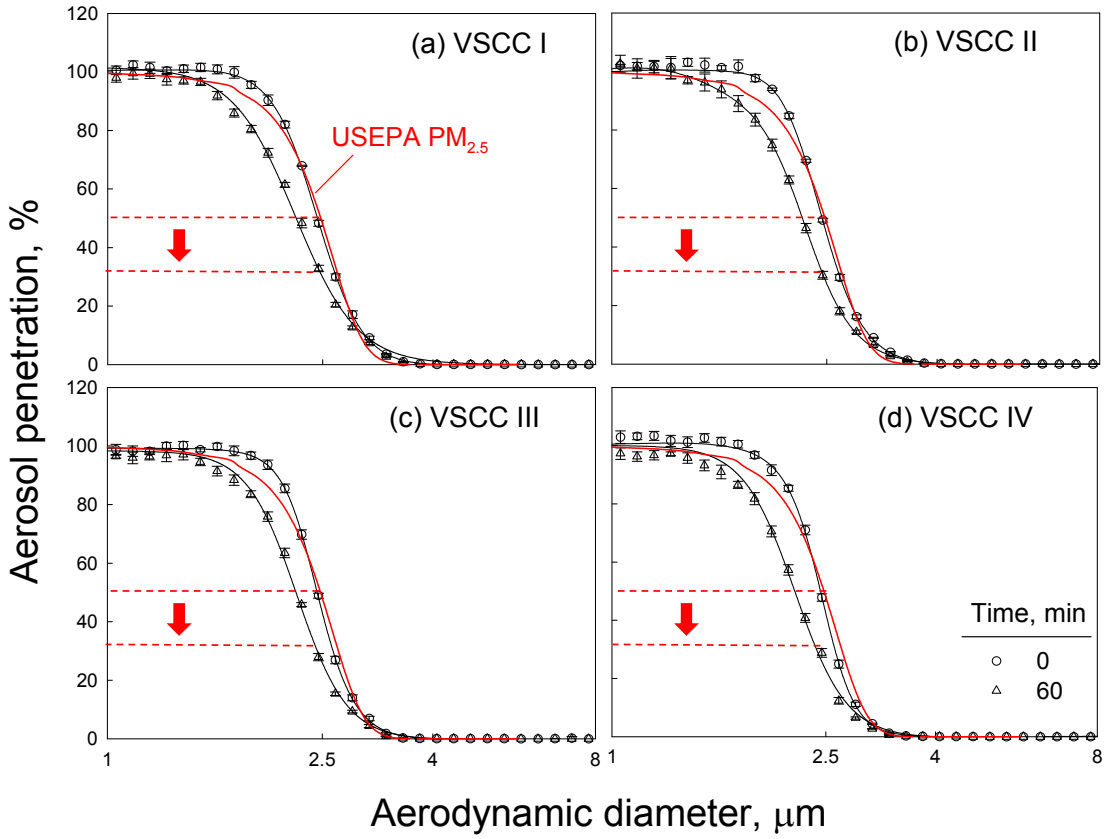

Fig. 7. Separation efficiency curves (initial and after one hour loading) for different-sized cyclones.

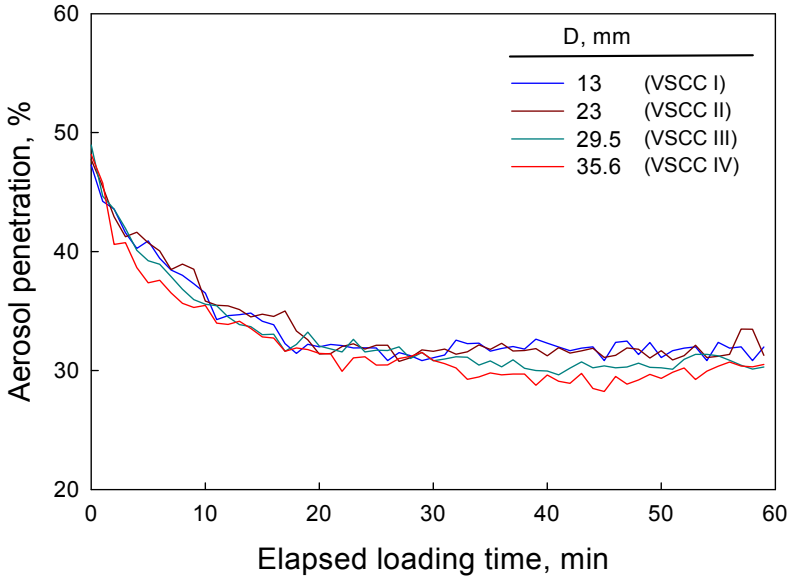

Fig. 8. Penetration of 2.5 μm PST particles through four different-sized cyclones as a function of loading time.

is far less than 1% of the air volume, so the aerosol is still mostly air. That means particles are far apart to have little effect on each other. Therefore, as a reasonable estimation, a daily cleaning is required when a cyclone is used as a separator for continuous $PM_{2.5}$ monitoring to prevent the sampling bias due to aerosol loading. However, it is inconvenient to clean the $PM_{2.5}$ sampler on a daily basis in continuous particulate monitoring. Therefore, it is necessary to find a $PM_{2.5}$ particle size separator free of aerosol loading effect and easy to maintain for continuous particulate matter monitoring, such as the water-film cleaning method to keep the impaction surface clean (Le and Tasi, 2017). The virtual cyclone, also referred to as anticyclone, which employs nonimpact aerosol separation, is proposed to meet

the requirements and further study on the optimization of the virtual cyclone for $PM_{2.5}$ sampling is ongoing.

Effect of Air Humidity on the Loading Characteristics

The hygroscopic behavior of particles on aerosol penetration is evaluated by challenging the cyclone with 3.6 mg m^{-3} PST particles with CMD of 3 μm and GSD of 1.27 under 20, 30, 50, 60, 80 and 90% RH. Fig. 9 shows initial aerosol penetration curves under varying air humidity from 20 to 90% RH and after-loading ones curves under 20 and 90% RH, respectively. The total loaded masses are 3.5 and 3.6 mg while the reductions of the 2.5-μm aerosol penetration under 20 and 90% RH are 19.5 ± 1.5% and 31.2 ± 2.2%, respectively. The after-loading cut-points shift from 2.5 μm to 2.25 and 2.10 μm for 20 and 90% RH, respectively. The separation curves after loading deviate from the $PM_{2.5}$ performance curve promulgated by the USEPA. The loading effect is observed for both low and high humidity conditions. Moreover, the aerosol penetration curves shift toward smaller sizes after particle loading, especially under high RH. This is speculated to be because water vapor condenses onto the particle surfaces, altering the surface properties of the challenge PST particles and increasing the adhesive force between incident particles and the impaction wall surface. As a result, the loading effect is more significant for cyclones operating under high humidity conditions. The CMDs of the challenged PST particles remain constant at 3.28 μm for RHs under 60% and then grow to 3.79 μm for RHs over 80% as shown in Fig. 10. The hysteresis behavior of PST particles over the

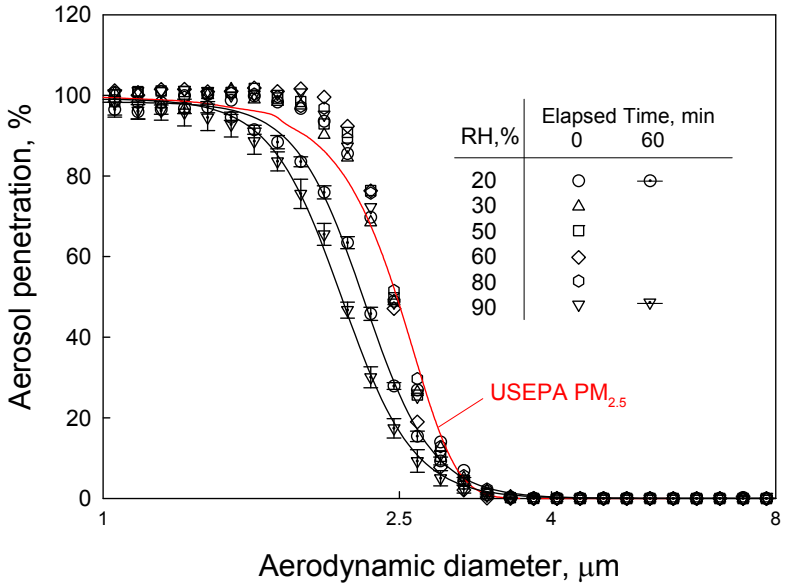

Fig. 9. Separation efficiency curves (initial and after one hour loading) under different relative humidities.

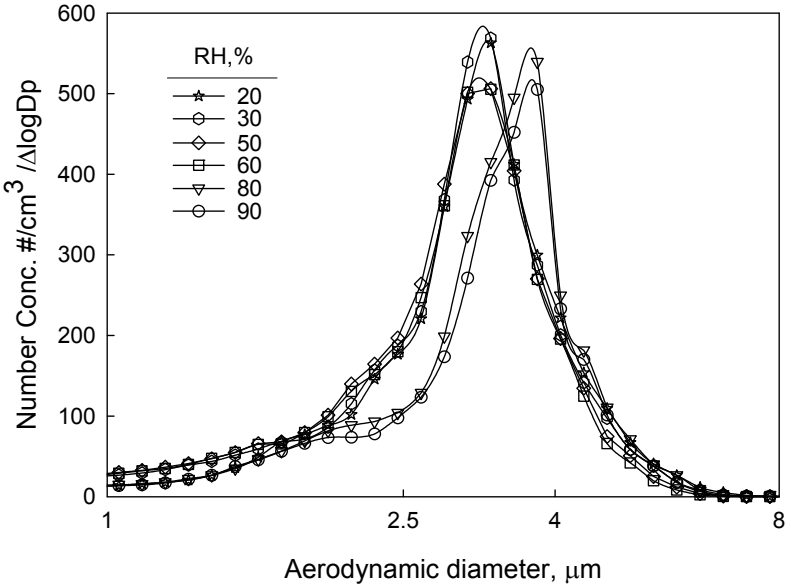

Fig. 10. Size distributions of PST particles under different air humidities.

deliquescence RH not only enlarges the PST particles but also significantly reduces the separation performance of cyclones with progressive aerosol loading.

CONCLUSIONS AND RECOMMENDATIONS

Of the two major types of USEPA designated $PM_{2.5}$ separators used in continuous particulate monitoring, cyclones provide better performance than impactors over long sampling periods with heavy loading. However, cyclones are still subject to the aerosol loading effect. This study provides comprehensive information on the impact of aerosol loading on cyclone performance. It is striking to find that the performance begins to deteriorate just as aerosol loading initiates. The aerosol-loading effect is complex, depending not only on the aerosol phase but also the particle materials. As expected, liquid aerosols such as DEHS particles have no observed loading effect, which is in good agreement with previous studies. The PST particles exhibit more of an impact on the cyclone performance with respect to aerosol loading.

Surprisingly, regardless of the higher loaded mass, larger solid particles have less of an effect than smaller ones on the cyclone performance. That is to say, the loading of particles with sizes close to the separator's cut-point has a more serious impact on the separation. The cyclone performance is further worsened by the high humidity over the deliquescence relative humidity of challenged particles. For the four different-sized cyclones that were studied, no significant difference in the loading characteristics can be found. Aerosol loading causes variations in the D_p50 cut-point and sharpness of the aerosol penetration curves, which deviate from the USEPA defined $PM_{2.5}$ sampling convention. As a result, the $PM_{2.5}$ mass concentration will be underestimated. Due to an abrupt decrease in the 2.5-μm aerosol penetration during the first 20 minutes of aerosol loading, a more limited range of precision in the published performance requirements regarding the D_p 50 for an FRM $PM_{2.5}$ sampler is advised. To accommodate successive $PM_{2.5}$ monitoring for a prolonged period of time, the use of a virtual cyclone without aerosol loading might be a feasible solution and is under investigation.

ACKNOWLEDGMENTS

This research was financially supported by the Ministry of Science and Technology, Taiwan, R. O. C., under the grants MOST 105-3011-F-273-001 and MOST 106-3011-F-273-001.

REFERENCES

Blachman, M.W. and Lippmann, M. (1974). Performance characteristics of the multicyclone aerosol sampler. *Am. Ind. Hyg. Assoc. J.* 35: 311–326.

Chen, C.C. and Huang, S.H. (1999). Shift of aerosol penetration in respirable cyclone samplers. *Am. Ind. Hyg. Assoc. J.* 60: 720–729.

Dockery, D.W., Pope, C.A., Xu, X., Spengler, J.D., Ware, J.H., Fay, M.E., Ferris, B.G.J. and Speizer, F.E. (1993). An association between air pollution and mortality in six U.S. cities. *New Eng. J. Med.* 329: 1753–1759.

Dominici, F., Peng, R.D., Bell, M.L., Pham, L., McDermott, A., Zeger, S.L. and Samet, J.M. (2006). Fine particulate air pollution and hospital admission for cardiovascular and respiratory diseases. *JAMA* 295: 1127–1134.

Hsu, C. W., Huang, S. H., Lin, C.W., Hsiao, T.C., Lin, W.Y. and Chen, C.C. (2014). An experimental study on performance improvement of the stairmand cyclone design. *Aerosol Air Qual. Res.* 14: 1003–1016.

Kenny, L.C. and Gussman, R.A. (1997). Characterization and modelling of a family of cyclone aerosol preseparators. *J. Aerosol Sci.* 28: 677–688.

Kenny, L.C., Merrifield, T., Mark, D., Gussman, R. and Thorpe, A. (2004). The development and designation testing of a new USEPA-approved fine particle inlet: A study of the usepa designation process. *Aerosol Sci. Technol.* 38: 15–22.

Kenny, L.C., Thorpe, A. and Stacey, P. (2017). A collection of experimental data for aerosol monitoring cyclones. *Aerosol Sci. Technol.* 51: 1–11.

Kim, K.H., Kabir, E., Kabir, S. (2015). A review on the human health impact of airborne particulate matter. *Environ. Int.* 74: 136–143.

Le, T.C. and Tsai, C.J. (2017). Novel non-bouncing $PM_{2.5}$ impactor modified from well impactor ninety-six. *Aerosol Sci. Technol.* 51: 1287–1295.

Okuda, T., Isobe, R., Nagai, Y., Okahisa, S., Funato, K. and Inoue, K. (2015). Development of a high-volume $PM_{2.5}$ particle sampler using impactor and cyclone techniques. *Aerosol Air Qual. Res.* 15: 759–767.

Ostro, B., Broadwin, R., Green, S., Feng, W.Y. and Lipsett, M. (2006). Fine particulate air pollution and mortality in nine California counties: Results from calfine. *Environ. Health Perspect.* 114: 29–33.

Tsai, C.J., Shiau, H.G., Lin, K.C. and Shih, T.S. (1999). Effect of deposited particles and particle charge on the penetration of small sampling cyclones. *J. Aerosol Sci.* 30: 313–323.

Vanderpool, R.W., Peters, T.M., Natarajan, S., Gemmill, D.B. and Wiener, R.W. (2001). Evaluation of the loading characteristics of the EPA WINS $PM_{2.5}$ separator. *Aerosol Sci. Technol.* 34: 444–456.

Xing, Y.F., Xu, Y.H., Shi, M.H. and Lian, Y.X. (2016). The Impact of $PM_{2.5}$ on the Human Respiratory System. *J. Thoracic Dis.* 8: E69–E74.

Zanobetti, A., Franklin, M., Koutrakis, P. and Schwartz, J. (2009). Fine particulate air pollution and its components in association with cause-specific emergency admissions. *Environ. Health* 8: 58–58.

Received for review, November 2, 2017
Revised, February 12, 2018
Accepted, February 15, 2018